

RESEARCH ARTICLE

Open Access



A Sox17 downstream gene *Rasip1* is involved in the hematopoietic activity of intra-aortic hematopoietic clusters in the midgestation mouse embryo

Gerel Melig¹, Ikuo Nobuhisa^{1,2*}, Kiyoka Saito¹, Ryota Tsukahara¹, Ayumi Itabashi¹, Yoshiakira Kanai³, Masami Kanai-Azuma⁴, Mitsujiro Osawa⁵, Motohiko Oshima⁶, Atsushi Iwama⁶ and Tetsuya Taga^{1*}

Abstract

Background During mouse embryonic development, definitive hematopoiesis is first detected around embryonic day (E) 10.5 in the aorta-gonad-mesonephros (AGM) region. Hematopoietic stem cells (HSCs) arise in the dorsal aorta's intra-aortic hematopoietic cell clusters (IAHCs). We have previously reported that a transcription factor Sox17 is expressed in IAHCs, and that, among them, CD45^{low}c-Kit^{high} cells have high hematopoietic activity. Furthermore, forced expression of Sox17 in this population of cells can maintain the formation of hematopoietic cell clusters. However, how Sox17 does so, particularly downstream signaling involved, remains poorly understood. The purpose of this study is to search for new Sox17 targets which contribute to cluster formation with hematopoietic activity.

Methods RNA-sequencing (RNA-seq) analysis was done to identify genes that are upregulated in Sox17-expressing IAHCs as compared with Sox17-negative ones. Among the top 7 highly expressed genes, *Rasip1* which had been reported to be a vascular-specific regulator was focused on in this study, and firstly, the whole-mount immunostaining was done. We conducted luciferase reporter assay and chromatin immunoprecipitation (ChIP) assay to examine whether Sox17 regulates *Rasip1* gene expression via binding to its enhancer element. We also analyzed the cluster formation and the multilineage colony-forming ability of *Rasip1*-transduced cells and *Rasip1*-knockdown Sox17-transduced cells.

Results The increase of the *Rasip1* expression level was observed in Sox17-positive CD45^{low}c-Kit^{high} cells as compared with the Sox17-nonexpressing control. Also, the expression level of the *Rasip1* gene was increased by the Sox17-nuclear translocation. *Rasip1* was expressed on the membrane of IAHCs, overlapping with the endothelial cell marker, CD31, and hematopoietic stem/progenitor marker (HSPC), c-Kit. *Rasip1* expression was observed in most part of c-Kit⁺Sox17⁺ cells in IAHCs. Luciferase reporter assay and ChIP assay indicated that one of the five putative Sox17-binding sites in the *Rasip1* enhancer region was important for *Rasip1* expression via Sox17 binding. *Rasip1* knockdown in Sox17-transduced cells decreased the cluster formation and diminished the colony-forming ability,

*Correspondence:

Ikuo Nobuhisa
nobuhisa@nakamura-u.ac.jp
Tetsuya Taga
taga.scr@mri.tmd.ac.jp

Full list of author information is available at the end of the article



© The Author(s) 2023. **Open Access** This article is licensed under a Creative Commons Attribution 4.0 International License, which permits use, sharing, adaptation, distribution and reproduction in any medium or format, as long as you give appropriate credit to the original author(s) and the source, provide a link to the Creative Commons licence, and indicate if changes were made. The images or other third party material in this article are included in the article's Creative Commons licence, unless indicated otherwise in a credit line to the material. If material is not included in the article's Creative Commons licence and your intended use is not permitted by statutory regulation or exceeds the permitted use, you will need to obtain permission directly from the copyright holder. To view a copy of this licence, visit <http://creativecommons.org/licenses/by/4.0/>.

while overexpression of Rasip1 in CD45^{low}c-Kit^{high} cells led to a significant but transient increase in hematopoietic activity.

Conclusions Rasip1 knockdown in Sox17-transduced CD45^{low}c-Kit^{high} cells displayed a significant decrease in the multilineage colony-forming ability and the cluster size. Rasip1 overexpression in Sox17-untransduced CD45^{low}c-Kit^{high} cells led to a significant but transient increase in the multilineage colony-forming ability, suggesting the presence of a cooperating factor for sustained hematopoietic activity.

Keywords Hematopoiesis, AGM, IAHC, HSC, Sox17, Rasip1

Background

During mouse ontogeny, fetal hematopoiesis is initiated from blood islands of the yolk sac that wraps around embryos [1], which is termed primitive hematopoiesis [2]. Definitive hematopoiesis is first detected around embryonic day (E) 10.5 in the aorta-gonad-mesonephros (AGM) region [3]. HSC-containing intra-aortic hematopoietic cell clusters (IAHCs) are found attached to the inside wall of the dorsal aorta [3] and arise from a specialized subset of the endothelium, the so-called hemogenic endothelium [4], which has the differentiation capacity to produce endothelial cells and hematopoietic cells [5]. Cells in IAHCs express various marker proteins. Among them, endothelial cell markers, such as vascular endothelial-cadherin (VE-cad) and CD31, are expressed on cells located on the vessel wall side of IAHCs. A hematopoietic cell marker CD45 is expressed on cells of the vessel lumen side of IAHCs, while a hematopoietic stem/progenitor cell (HSPC) marker c-Kit is expressed on cluster cells [5–8]. HSCs emerge from vascular endothelial cells across the intra-arterial clusters, and Runx1 function is essential in endothelial cells for hematopoietic progenitor and HSC formation [9]. Mice deficient in the Runx1 transcriptional factor, which is essential for definitive hematopoiesis, show no such cell clusters in the dorsal aorta at midgestation of mouse embryo [5, 8]. These expression patterns of marker proteins in IAHCs imply that specification of the hematopoietic lineage occurs within the cell cluster [10].

The expression of CD45 is generally recognized as a marker of all hematopoietic cells except for mature erythrocytes and platelets. CD45 is used, in some cases together with a hematopoietic stem/progenitor cell (HSPC) marker c-Kit, to fractionate hematopoietic stem/progenitor cells (HSPCs) in the AGM region at midgestation. In previous studies, populations with negative and low-level CD45-expression have long-term repopulating activity [6], whereas the CD45-expressing population has differentiation ability [11, 12]. Our previous studies [13, 14] showed that the cells in the primary culture of dissociated AGM regions [15], which appears to be an *in vitro* reproduction of hematopoiesis in the AGM region, can be separated into at least CD45^{low}c-Kit⁺,

CD45^{low}c-Kit⁻, and CD45^{high}c-Kit^{low/-} populations based on the expression profile of CD45 and c-Kit [13, 14]. The CD45^{low}c-Kit^{high} cells have the highest hematopoietic capacity *in vitro* and long-term reconstituting ability *in vivo* [16]. Then, the hematopoiesis in the AGM region rapidly decreases later than E11.5 and disappeared at E13.5, and the main site of hematopoiesis shifts to the fetal liver at E12.5 [16, 17].

An endodermal transcription factor, Sry-related high-mobility-group (HMG) box 17 (Sox17), and also the other F-group (SoxF) proteins, Sox7 and Sox18, were expressed in E10.5 IAHCs [10]. Sox17, which is a marker of endodermal cells and a transcriptional regulator containing a DNA-binding domain, called the HMG box [18, 19]. Sox17-deficient embryos have a defect in tube formation of the endodermal-derived gut and are lethal at midgestation [20]. Sox17 is expressed in cells occupying the vessel wall side of the hematopoietic cell cluster in the dorsal aorta, which is specifically expressed in endothelial cells [10, 21]. Also, mouse embryonic stem (ES) cell analysis showed that enforced Sox17-expressing cells in embryonic bodies (EBs) differentiate into hemogenic endothelial cells and hematopoietic cells [10]. Conditional knockout mice lacking Sox17 demonstrated that Sox17 is important for fetal hematopoiesis, but not adult hematopoiesis [16]. Sox17⁺VE⁺ cells from the E11.5 AGM region showed multilineage hematopoietic reconstitution in mice [21]. These expression patterns imply that Sox17 regulates the development of the early stages of HSPCs. We have previously reported that the CD45^{low}c-Kit^{high} cell population in the E10.5 AGM region although minor in size displays the highest hematopoietic activity among all the populations classified by CD45 and c-Kit expression levels [16]. Forced expression of Sox17 in E10.5 AGM CD45^{low}c-Kit^{high} cells led to the consistent formation of cell clusters *in vitro* during at least 8 passages of co-cultures with stromal cells. In contrast, the knockdown of Sox17 in the Sox17-transduced cells led to dispersed hematopoietic colonies containing granulocytes and macrophages in the co-culture with stromal cells [10]. These reports suggest that Sox17 contributes to the maintenance of cells with stem cell phenotypes in the

hematopoietic cell clusters of the AGM region, and that the downregulation of Sox17 induces hematopoietic differentiation [10].

The Notch signaling pathway plays a significant role in fetal hematopoiesis. Notch1-knockout mouse embryos were found to be defective for definitive hematopoiesis and abnormal vascular formation [22]. Studies show that Sox17 interacts directly with the promoter region of Notch 1 and induces the expression of Notch1, followed by the Hes1 induction [17, 23]. The Sox17-Notch1-Hes1 axis is suggested to play a role in the maintenance of the undifferentiated state in Sox17-transduced cells [17, 23]. Moreover, the thrombopoietin (TPO) signaling pathway is important for the formation of Sox17-transduced IAHCs that highly express the TPO receptor c-Mpl and the maintenance of hematopoietic activity. The expression of c-Mpl was observed in IAHCs of E10.5 embryos, and the stimulation of the TPO leads to the emergence of hematopoietic cells from the endothelial cells of the AGM region [24].

Up until now, we have shown that the introduction of Sox17 in IAHC cells in the AGM region results in the formation of cell clusters with hematopoietic potential [10, 17, 23–25] and assume that Sox17 induces the expression of target genes to maintain an undifferentiated state via the interaction of Sox17 with its promoter. Such genes include Notch1 [17], ESAM, and VE-Cad [23], and each gene induced by Sox17 may have distinct functions in the maintenance of undifferentiated states. However, it remains to be determined how these genes function to confer cluster formation and hematopoietic activity by the Sox17 and whether there still are unidentified Sox17 target genes. In the present study, RNA-seq analysis was done to identify genes that are upregulated in the Sox17-expressing IAHCs from the 10.5 AGM region as compared with Sox17-nonexpressing ones, according to the method by Kayamori et al. [26] with the use of mice carrying the enhanced GFP gene in frame with Sox17 start codon [27, 28]. In this study, we focus on the *Rasip1* gene because, among the top 7 highly expressed genes, *Rasip1* was reported to be a vascular-specific regulator but not recognized as a hematopoietic regulator. We here further show the functional role of *Rasip1* in the maintenance of HSC-containing IAHC cells of the E10.5 AGM region.

Methods

Animals

ICR mice were purchased from Japan SLC. Animal experiments were performed by institutional guidelines approved by the Animal Care Committee of Tokyo Medical and Dental University (approval number: A2018-265C, A2019-108C, A2021-177C, A2023-146A).

Isolation of IAHCs from the AGM region

AGM regions excised from E10.5 ICR mice were incubated in 1 mg/ml Dispase II (Roche, Basel, Switzerland) for 20 min at 37 °C. After washing cells with stop solution [Hank's balanced salt solution (HBSS) containing 10% (v/v) fetal calf serum (FCS) and 250 µg/ml DNase I (Roche)], cells were resuspended in Dulbecco's modified Eagle's medium (DMEM) containing 2% (v/v) FCS. The cells were subjected to immunostaining with phycoerythrin (PE)-conjugated anti-mouse CD45 (30-F11) and allophycocyanin (APC)-conjugated anti-mouse c-Kit (2B8) antibodies (eBioscience, San Diego, CA, USA). Stained cells were suspended in DMEM supplemented with 2% (v/v) FCS and 1 µg/ml propidium iodide (PI) (Calbiochem, Darmstadt, Germany) and analyzed by FACS Aria II (Becton Dickinson, Lincoln, NJ, USA). The results of flow cytometry were analyzed with FlowJo (Three Star Inc., Ashland, VT, USA). Sorted CD45^{low}c-Kit^{high} cells seeded on OP9 stromal cells in an alpha-minimal essential medium (α-MEM) supplemented with 10% (v/v) FCS, 25 ng/ml stem cell factor (SCF, PeproTech, Rocky Hill, NJ), 10 ng/ml interleukin-3 (IL-3, PeproTech), and 10 ng/ml thrombopoietin (TPO, PeproTech).

RNA-seq analysis

RNA-seq analysis was done as described previously [26]. We used the AGM region of heterozygous embryos, in which the Sox17 gene was replaced with the enhanced GFP gene [27, 28]. Total RNA was isolated from the E10.5 Sox17 (GFP)⁺ mouse AGM region-derived CD45^{low}c-Kit^{high} cells treated with DMSO, 30 nM of PTC299, 200 nM of decitabine, and a combination of both agents using the RNeasy Mini Kit (Qiagen). After reverse transcription, the libraries for RNA-seq were generated from fragmented DNA using a Next Ultra DNA Library Prep Kit (New England BioLabs). After the quantification of the libraries by TapeStation (Agilent), samples were subjected to sequencing with HiSeq1500 (Illumina). RNA-seq raw reads (fastq files) were mapped to a mouse genome. Gene level counts for fragments mapping uniquely to the mouse genome were extracted from BAM files. Gene expression values were then calculated as reads per kilobase of exon units per million mapped reads using cuff links (version 2.2.1). Table S1 describes expression levels of genes examined in Sox17 (GFP)⁺ CD45^{low}c-Kit^{high} cells and Sox17 (GFP)⁻ CD45^{low}c-Kit^{high} cells from the same set of E10.5 Sox17-GFP embryos. In this table, the values of FPKM+1 were used to calculate the ratio of gene expression levels between the Sox17 (GFP)⁺ CD45^{low}c-Kit^{high} cells and the Sox17 (GFP)⁻ CD45^{low}c-Kit^{high} cells. The genes are listed

Table 1 Top 7 selected genes expressed at high levels in Sox17 (GFP)⁺ CD45^{low}c-Kit^{high} cells of E10.5 Sox17-GFP embryo as compared with Sox17 (GFP)⁻ CD45^{low}c-Kit^{high} cells. FPKM, fragments per kilobase of transcript per million mapped reads. In this table, the values of FPKM + 1 were used to calculate the ratio of gene expression levels between the Sox17 (GFP)⁺ CD45^{low}c-Kit^{high} cells and the Sox17 (GFP)⁻ CD45^{low}c-Kit^{high} cells from the same set of E10.5 Sox17-GFP embryos

		Sox17 ⁺ (FPKM + 1)/ Sox17 ⁻ (FPKM + 1)
1	<i>Cldn5</i>	242.21
2	<i>Sox18</i>	126.71
3	<i>Aplnr</i>	121.16
4	<i>Esam</i>	87.78
5	<i>Rasip1</i>	75.09
6	<i>Plvap</i>	69.84
7	<i>Emcn</i>	62.70

according to the ratio of the former to the latter. Table 1 shows the top 7 selected genes from Table S1.

Retroviral transduction of genes into cells

Plat-E cells for packaging ectopic retroviruses [29] were seeded 1 day before transfection. pMY vector inserted with a gene of interest was transfected into PlatE packaging cells with Trans IT-293 Reagent (Mirus, Madison, WI, USA). After 2 days of culture, the culture medium containing retroviruses was collected. CD45^{low}c-Kit^{high} cells sorted from the E10.5 AGM region were infected with retroviruses encoding the Sox17-, Sox17-ERT-, Rasip1-internal ribosomal entry sequence (IRES)-GFP, or the Sox17-IRES-mCherry gene in the presence of 10 µg/ml polybrene at 37 °C for 2.5 h. Transduced cells were co-cultured with OP9 stromal cells in α-MEM containing 10% FCS, 25 ng/ml SCE, 10 ng/ml IL-3, and 10 ng/ml TPO.

Tamoxifen-dependent nuclear translocation of Sox17 and analysis of Rasip1 expression

The Sox17-ERT-IRES-GFP-encoding retrovirus was infected with CD45^{low}c-Kit^{high} cells from the E10.5 AGM region [30]. The transduced cells were co-cultured with OP9 stromal cells supplemented with SCE, IL-3, and TPO with or without tamoxifen (1 µg/ml tamoxifen citrate). After 3 days of culture, Sox17-ERT-IRES-GFP-transduced cells were sorted by flow cytometry. cDNA was synthesized from total RNA isolated from sorted cells, and Rasip1 expression was analyzed by RT-PCR.

Whole-mount immunostaining

Whole-mount immunostaining was performed according to a previously described protocol [5, 17, 23]. E10.5 ICR mouse embryos were fixed in 2% paraformaldehyde (PFA) for 20 min on ice. After washing with PBS, the embryos were treated with PBS-MT [1% (w/v) skim milk powder, and 0.4% (v/v) Triton X-100] containing 2% (w/v) bovine serum albumin for 1 h on ice, and then immunostained with a rat anti-mouse CD117 (c-Kit) antibody (2B8; BD Pharmingen), a goat anti-mouse CD31 antibody (Bio-Techne, Minneapolis, MN, USA), and a rabbit anti-mouse Rasip1 antibody (Proteintech, Rosemont, IL, USA) overnight at 4 °C. Immunostained embryos were washed three times with PBS-MT for 1 h each and then stained with Alexa Fluor 647-conjugated donkey anti-rat IgG (Jackson ImmunoResearch, West Grove, PA, USA), Alexa Fluor 546-conjugated donkey anti-goat IgG (Invitrogen, Oregon, USA), and Alexa Fluor 488-conjugated donkey anti-rabbit IgG (Invitrogen). Embryos were in some experiments co-immunostained with a rat anti-mouse CD117 (c-Kit) antibody (eBioscience), a rabbit anti-mouse Rasip1 antibody (Proteintech), and a goat antihuman Sox17 antibody (R&D Systems, Minneapolis, MN, USA) overnight at 4 °C. It is indicated in the R&D Systems' datasheet that the goat antihuman Sox17 antibody clearly detects mouse Sox17 protein in the B16 mouse melanoma cell line. This antibody has also been reported to efficiently recognize Sox17 protein in mouse embryo [10, 23]. After washing three times, these embryos stained with Alexa Fluor 647-conjugated donkey anti-rat IgG (Jackson ImmunoResearch), Cy3-conjugated donkey anti-rabbit IgG (Jackson ImmunoResearch), and Alexa Fluor 488-conjugated donkey anti-goat IgG (Invitrogen) in PBS-MT overnight at 4 °C. After washing three times with PBS-MT for 1 h each, embryos were stained with Hoechst 33,258 (Nacalai Tesque, Kyoto, Japan) in PBS-T (0.4% [v/v] Triton X-100 in PBS) for 20 min at 4 °C, followed by washing twice with PBS-T for 20 min each at 4 °C. Moreover, embryos were treated with 50% (v/v) methanol/PBS for 10 min at 4 °C and then treated twice with 100% methanol for 10 min each at 4 °C. The embryos were washed in a 50% (v/v) methanol/a mixture of benzyl alcohol and benzyl benzoate (1:2, BABB) three times. Finally, the embryos were mounted in BABB. Observations were performed by confocal laser-scanning microscopy (LSM 510; Carl Zeiss, Oberkochen, Germany).

Luciferase assay

NIH3T3 cells (1.0 × 10⁶) were transduced with a pEF-BOSE vector encoding Sox17, Sox17G103R mutant, which disrupts the DNA-binding capacity, pGL3

vector (Promega, Madison, WI, USA) carrying the putative Rasip1 enhancer or point-mutated Rasip1 enhancers and pRL-CMV or pRL-TK encoding sea pansy luciferase genes with Trans-IT LT1 reagent (Mirus, Madison, WI, USA). After 3 days, cells were solubilized, and luciferase activities in cell lysates were monitored by the Dual-Luciferase Reporter Assay System (Promega), and a Mithras LB 940 (Berthold Technologies, Bad Wildbad, Germany) was used for quantitation. First, the pRL-CMV vector (Promega) and Sox17G103R mutant were used in the control luciferase assay. Then, the pRL-TK vector (Promega) was mainly used in the luciferase assay.

Chromatin immunoprecipitation (ChIP) assay

ChIP assay was performed using ChIP-IT Express Enzymatic Kit (Active Motif, Carlsbad, CA, USA). The *Sox17-IRES-GFP* gene was retrovirally transduced into sorted CD45^{low}c-Kit^{high} cells from E10.5 mouse embryos. The transduced cells were co-cultured with OP9 cells, and after 4 days of incubation, these cells were reseeded onto new OP9 stromal cells. After several passages, Sox17-transduced cells (1.2×10^8 cells) were harvested and fixed with 1% formaldehyde solution (37% formaldehyde, Sigma Aldrich, St. Louis, USA) in 20 ml α MEM for 10 min. After 2 times washing with PBS, the cells were treated with lysis buffer supplemented with a protease inhibitor cocktail and PMSF (ChIP-IT Express Enzymatic Kit, Active Motif). Next, cells were homogenized by Dounce homogenizer, and the nuclei preparation was treated with Digestion Buffer supplemented with a protease inhibitor cocktail and PMSF (ChIP-IT Express Enzymatic Kit, Active Motif). Then, enzymatic digestion of chromatin was performed by using enzymatic shearing cocktail (ChIP-IT Express Enzymatic Kit, Active Motif) for 5 min at 37 °C and was stopped with the addition of cold EDTA. This enzyme-digested chromatin sample was subjected to RNAase and proteinase K treatment (ChIP-IT Express Enzymatic Kit, Active Motif), and phenol/chloroform extraction, followed by DNA precipitation as described in the protocol. An aliquote of the sample was separated by electrophoresis through a 1% agarose gel to check the presence of optimally digested DNA. Then, the remaining sample was mixed with radioimmunoassay-grade BSA (Wako, Osaka, Japan)-coated Protein G magnetic beads (ChIP-IT Express Enzymatic Kit, Active Motif) and either normal goat IgG control (R&D Systems) or a goat anti-human Sox17 antibody (R&D Systems) overnight. After washing the magnetic beads with ChIP buffer (ChIP-IT Express Enzymatic Kit, Active Motif), the immunoprecipitated chromatin was eluted with elution buffer and subjected to reverse-cross-linking and proteinase K treatment (ChIP-IT Express Enzymatic Kit, Active Motif). Purified DNA fragments were

amplified by PCR with the following primers: Sox17-binding sense, 5'-CATATGACAAGTCTGGTAGCC-3', and antisense, 5'-ACATCGCCAATACTTGTATCTG-3'.

Knockdown of Rasip1 in CD45^{low}c-Kit^{high} cells prepared from the E10.5 AGM region

The shRNA sequences and hairpin oligonucleotides designed with 9-mer nucleotide spacer TTCAAGAGA [31] were annealed downstream of the U6 promoter in the pMKO. shRNA sequences were as follows: 5'-GCTTGAAACTGCATCGCTT-3' (shRasip1) and 5'-ACTTACGCTGAGTACTTCG-3' (shLuc). In the same retrovirus vector containing U6 promoter-shRasip1 or shLuc, a GFP gene was expressed under the control of the SV40 promoter [9]. The shRNA and GFP constructs were introduced into Sox17-IRES-mCherry-transduced cells derived from the E10.5 CD45^{low}c-Kit^{high} cells by a retrovirus, followed by co-culture with OP9 cells for 4 days. After 4 days of co-culture, Sox17-IRES-mCherry-transduced cells formed clusters that expressed bright GFP (shRNA). And the images of these clusters were taken with fluorescent microscopy. The volume of each Mock- and shRNA-transduced cell cluster was evaluated by the formula described by Wu et al. [32]. Cluster volume = length \times width²/2, where length represents the largest diameter and width represents the perpendicular diameter to the largest diameter. We then sorted GFP⁺ cells and assessed the colony-forming ability (2.5×10^3 GFP⁺ cells) after 7 days of the culture in a semisolid medium (Methocult M3434, Stem Cell Technologies, Vancouver, Canada) and the expression level of Rasip1 (2.0×10^4 GFP⁺ cells) using RT-PCR. Rasip1 KD efficiency was assessed by ImageJ and expressed in percentage as compared with β -actin expression.

Reverse transcription-polymerase chain reaction (RT-PCR)

Sorted cells were dissolved in ISOGEN (WAKO, Osaka, Japan), and RNAs were recovered according to the manufacturer's protocol. Then, cDNA was synthesized from total RNA isolated from sorted cells. Expression values for the Rasip1 knockdown or overexpression of the *Rasip1* gene were normalized to the levels of the β -actin gene. PCR amplification was performed using rTaq (TAKARA Bio Inc., Otsu, Japan) under the following conditions: 96 °C for 3 min and then cycles of 96 °C for 30 s, 55 °C for 30 s, and 72 °C for 30 s. The primer sets used were as follows:

- 5'-GTGACAGATGACGCATTGCATAGAGAA-3'
- 3'-ACTCAAACCTCTCAGCCGTCTACGCAGG-5' (Rasip1)
- 5'-CCAGGGTGTGATGGTGGGAA-3'; 3'-CAGCCTGGCTGGCTACGTACA-5' (β -actin)

Overexpression of Rasip1 in CD45^{low}c-Kit^{high} cells prepared from the E10.5 AGM region

A full-length cDNA encoding Rasip1 was inserted into the pMY-IRES-GFP vector with a FLAG-tag. FACS-sorted CD45^{low}c-Kit^{high} cells prepared from E10.5 AGM regions were infected with the retroviruses encoding the Rasip1-IRES-GFP gene in the presence of 10 mg/ml polybrene for 2.5 h. After 4 days of culture on OP9 stromal cells, GFP-encoding virus-infected cells were sorted by FACS Aria II and reseeded onto new OP9 stromal cells to proliferate the Rasip1-transduced cells. The process was repeated every 3 or 4 days.

Statistical analysis

All data of luciferase activities and colony counts are represented as the mean \pm standard deviation. Comparisons between the two samples were performed using Student's *t*-tests.

Results

Rasip1 is expressed in endothelial cells and cell membrane site of IAHCs of the E10.5 AGM region

We have previously reported that the CD45^{low}c-Kit^{high} cell population in the E10.5 AGM region has the highest hematopoietic activity among all the populations classified by CD45 and c-Kit expression levels [23]. Furthermore, we have demonstrated the forced expression of the transcription factor Sox17, which was previously suggested to maintain the hematopoietic activity in fetal hematopoiesis in E10.5 AGM CD45^{low}c-Kit^{high} cells, leads to the consistent formation of cell clusters with hematopoietic activity in vitro [10]. In the present study,

we first compared gene expression levels in Sox17 (GFP)⁺ CD45^{low}c-Kit^{high} cells and Sox17 (GFP)⁻ CD45^{low}c-Kit^{high} cells of the AGM regions of E10.5 Sox17 promoter-GFP knock-in embryos using RNA-seq analysis. Table 1 indicates the top 7 highly expressed genes that are likely to be transcriptional targets of Sox17. Within these top 7 genes that are highly expressed in Sox17 (GFP)⁺ CD45^{low}c-Kit^{high} cells, *Rasip1* is the least studied gene in murine embryonic hematopoiesis. Therefore, and because Rasip1 was reported to be a vascular-specific regulator, we focused on the involvement of the *Rasip1* gene in the formation of cluster cells in the E10.5 AGM region. Rasip1 is a protein that acts as a vascular-specific regulator of GTPase signaling, cell architecture, adhesion, and tubulogenesis [33–36]. As shown in Fig. 1A (lower panel), Rasip1 was expressed in endothelial cells and CD45^{low}c-Kit^{high} cells.

We have previously demonstrated the expression of Sox17 in basal cells of the E10.5 AGM region's IAHCs by whole-mount in situ hybridization, and CD45^{low}c-Kit^{high} cells transduced with Sox17 maintain their undifferentiated state [4]. Rasip1 expression in IAHCs of wild-type (WT) embryos was examined by immunohistochemistry. As shown in Fig. 1B, immunoreactivity for Rasip1 was detected in the membrane of c-Kit⁺ IAHC cells along with that for the endothelial cell marker CD31 expression. We observed Rasip1 expression in the aortic endothelium of the AGM region as well as the IAHC cell membrane site. Whole-mount immunostaining with antibodies to Rasip1, c-Kit, and Sox17 as shown in Fig. 1C indicates that Rasip1 is expressed in most part of the c-Kit⁺ and Sox17⁺ IAHC cells.

(See figure on next page.)

Fig. 1 Rasip1 expression in IAHCs in the E10.5 AGM region. **A** Upper panel: The expression profile of CD45, c-Kit, CD31, and VE-Cad in the E10.5 AGM region. The numbers from 1 to 4 indicate cell populations separated by the expression profile: (1) CD45⁻c-Kit⁻CD31⁺VE-cad⁻ cells (endothelial cells); (2) CD45⁻c-Kit⁻CD31⁺VE-cad⁺ cells (endothelial cells); (3) CD45^{low}c-Kit^{high} cells (containing HSPCs); (4) CD45⁺c-Kit⁻ cells (hematopoietic cells). Lower panel: RT-PCR shows the relative expression levels of *Rasip1* in these 4 populations. **B** Whole-mount immunofluorescence staining of Rasip1 (green), CD31 (red), and c-Kit (cyan) in IAHCs of the E10.5 AGM region. The Rasip1 expression on the membrane of IAHCs. The nuclei were stained by Hoechst 33,258 (blue). Scale bar, 20 μ m. **C** Whole-mount immunofluorescence staining of Sox17 (green), Rasip1 (red), and c-Kit (cyan) in IAHCs of the E10.5 AGM region. The nuclei were stained by Hoechst 33,258 (blue). Rasip1 is expressed in most part of c-Kit⁺ Sox17⁺ cells in IAHCs. Scale bar, 20 μ m. **D** A genetic scheme showing the location of the *Rasip1* gene and upstream genes in mouse chromosome 7.5 putative Sox17-binding sites were indicated by squares with numbers 1 through 5. Upper panel: Requirement of the proximal putative Sox17-binding site (5) for induction of the Rasip1 gene by Sox17. NIH3T3 cells (1×10^6) were transfected with a pGL3 vector containing the putative Rasip1 enhancer sequences. pRL-CMV was co-transfected as an internal control. The region Rasip1 [1-3] (979 bp) has three putative Sox17-binding sites (1, 2, and 3), and the region Rasip1 [2-3] (602 bp) has two putative Sox17-binding sites (2 and 3). The region Rasip1 [4-5] (720 bp) has putative Sox17-binding sites 4 and 5. Two types of Sox17-binding sites are shown in the enhancer regions: (1) AATGGCG (Sox17-binding sites 2, 4) and (2) ATGTG (Sox17-binding sites 1, 3, 5). Lower panel: Inhibition of the Sox17-induced *Rasip1* gene activation by a mutation in the putative Sox17-binding site 5. NIH3T3 cells (1×10^6) were transfected with a pGL3 vector containing the putative Rasip1 enhancer sequences with point mutations in the putative Sox17-binding sites 4 or 5, or both together with plasmids encoding wild-type (WT) Sox17 or Sox17G103R which lost the DNA binding ability. In this experiment, pRL-TK was co-transfected as an internal control. A solid black line indicates the Rasip1 [4-5] region, solid grey lines show the pGL3 vector and Rasip1 enhancer region [1-3] as controls. **E** Enzyme-digested chromatin-derived DNA. DNA from the enzyme-digested chromatin was analyzed by electrophoresis. Two bars on the right show the presence of optimally digested DNA. **F** ChIP assay. The digested chromatin sample was immunoprecipitated with either the anti-Sox17 antibody or normal goat IgG. DNA samples from the immunoprecipitates were subjected to PCR to amplify the region containing the Sox17-binding site 5 (Rasip1 [5]; see Fig. 1D top diagram). The expected PCR fragment length is 223 bp. Similar results were obtained by 2 independent sets of PCR amplifications of the samples from 2 independent preparations of cells from separately obtained E10.5 embryos purchased on different days

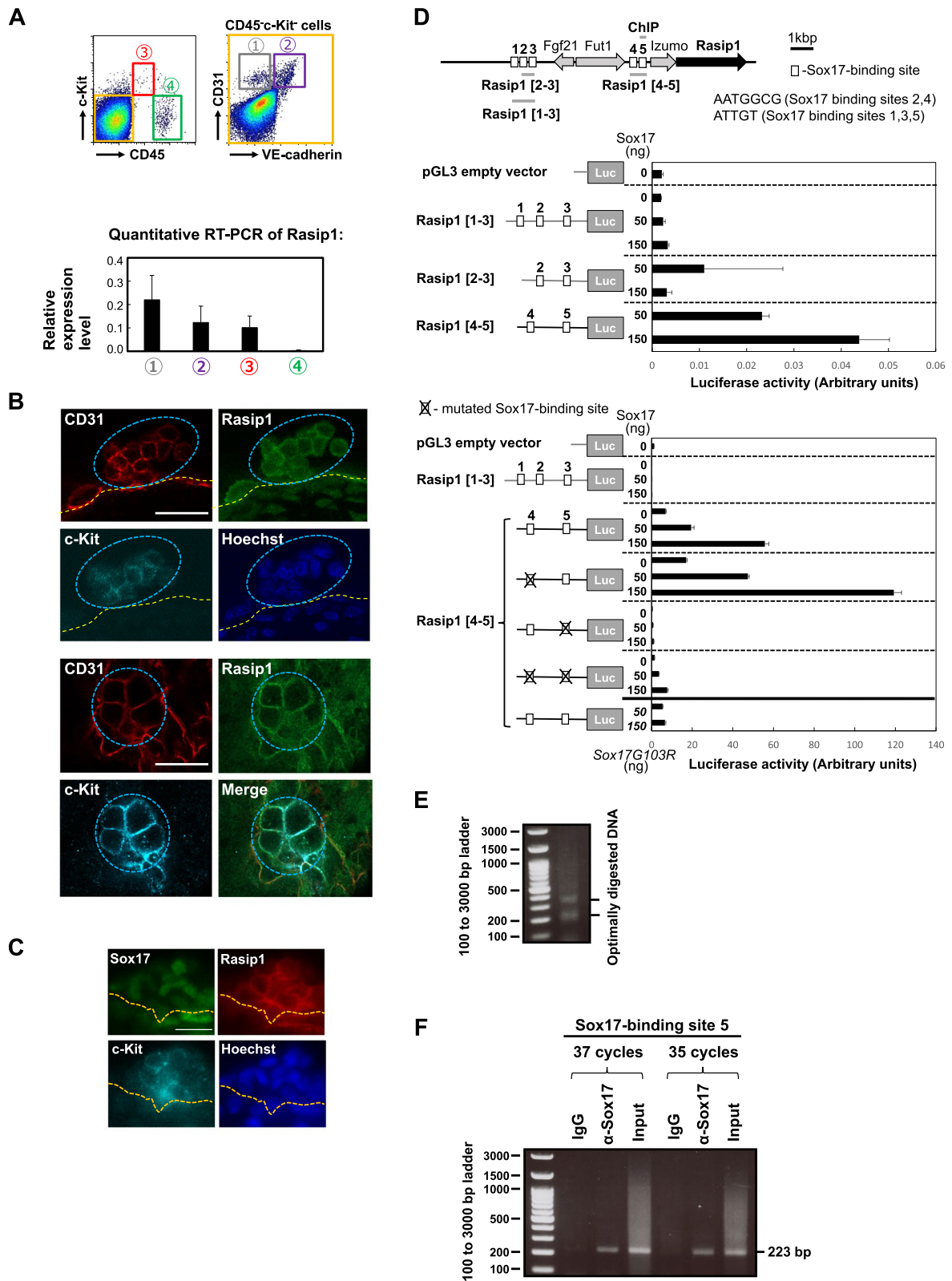


Fig. 1 (See legend on previous page.)

To evaluate the effect of Sox17 on the *Rasip1* activation, we first searched for the putative Sox17-binding site in the upstream region of the *Rasip1* gene. Five putative Sox17-binding sites were observed in the region (Fig. 1D). We examined the luciferase activity of the enhancer constructs, in which *Rasip1* [1–3] contained the first three putative Sox17-binding sites, *Rasip1* [2, 3] included the second and the third putative Sox17-binding sites, and *Rasip1* [4, 5] had the other two putative Sox17-binding sites, with the varying amount of vector encoding the Sox17 or its mutant with no DNA-binding capacity (Fig. 1D). As shown in Fig. 1D (upper panel), the introduction of Sox17 led to increased *Rasip1* enhancer activity of the *Rasip1* [4, 5] construct in a dose-dependent manner. In contrast, the Sox17G103R mutant, in which Gly¹⁰³ is replaced with Arg to disrupt its DNA-binding activity, did not induce the luciferase activity of the putative *Rasip1* enhancer region, *Rasip1* [4, 5] (Fig. 1D, lower panel, the bottom pair of bars). Moreover, the *Rasip1* enhancer activity of the *Rasip1* [4, 5] construct decreased abruptly when the Sox17 protein was absent or had a nonfunctioning mutation, or a putative Sox17-binding site 5 in the *Rasip1* gene was mutated (Fig. 1D, lower panel). These data suggest that Sox17 binds to the *Rasip1* enhancer region and induces expression of the *Rasip1* gene.

Next, we performed a ChIP assay to examine whether Sox17 binds to the Sox17-binding site 5 in the *Rasip1* gene enhancer region. For this purpose, the *Sox17-IRES-GFP* gene was retrovirally introduced into CD45^{low}c-Kit^{high} cells of E10.5 mouse embryos, and cluster-forming cells with hematopoietic activity were expanded by several passages, as in the case of some other key experiments in this study. The cells were homogenized by Dounce homogenizer, and the nuclei preparation was subjected to enzymatic digestion of chromatin as described in “Methods.” Fig. 1E (two bars on the right) shows the presence of optimally digested DNA as indicated by the manufacturer’s procedure (ChIP-IT Express Enzymatic Kit, Active Motif) and based on the reported length of the nucleosomal DNA (147 bp) and the linker DNA (about 45 bp) between nucleosomes [37]. Then, the digested chromatin samples were immunoprecipitated with anti-Sox17 antibody or normal IgG. DNA fragments from the immunoprecipitates were subjected to PCR to analyze the binding of Sox17 to the Sox17-binding site 5 in the *Rasip1* gene enhancer region. As shown in Fig. 1F, the PCR product of the expected size was obviously present in the DNA sample precipitated with anti-Sox17 antibody, whereas that was not detectable in the sample precipitated with control IgG, indicating that Sox17 interacts with the Sox17-binding site 5.

Rasip1 is expressed in Sox17-transduced CD45^{low}c-Kit^{high} cells with high hematopoietic activity

We previously showed that when CD45^{low}c-Kit^{high} cells sorted from E10.5 AGM regions were transduced with Sox17-IRES-GFP virus and co-cultured with OP9 stromal cells with SCF, IL3, and TPO; the Sox17-transduced cells formed cell clusters with high hematopoietic activity [4]. We thus examined the expression level of *Rasip1* in Sox17-transduced CD45^{low}c-Kit^{high} cells by RT-PCR analysis. As shown in Fig. 2A, the *Rasip1* gene was clearly expressed in Sox17-transduced cells, while its expression was almost negligible in the mock-transduced cells. This result indicates that the *Rasip1* gene is a target of Sox17 and implies that *Rasip1* may contribute to the Sox17-transduced cell cluster formation.

Next, we examined the *Rasip1* expression level in Sox17-ERT-transduced CD45^{low}c-Kit^{high} cells sorted from E10.5 AGM by RT-PCR analysis. Tamoxifen is a reagent that dose dependently transports the Sox17-ERT fusion protein into the nucleus of the cells. As shown in Fig. 2B, tamoxifen-dependent nuclear import of Sox17-ERT proteins in the CD45^{low}c-Kit^{high} cells led to an increased expression level of *Rasip1* compared to the control. Together, these results are in agreement with those of the luciferase assay and the ChIP assay, implying that the Sox17 transcription factor is tightly associated with the induction of *Rasip1* expression.

Rasip1 knockdown in Sox17-transduced cluster cells impedes cluster formation and decreases the hematopoietic activity

To confirm the contribution of *Rasip1* to the formation of cell clusters with high hematopoietic activity, retroviruses encoding shRNA against luciferase (shLuc) and *Rasip1* (sh*Rasip1*) and a GFP gene were infected with Sox17-transduced cells. After 4 days of the culture with the stromal cells, we found that most of the cells express mCherry, i.e., Sox17 (Fig. 3A, lower left panel). This is because, without Sox17, AGM cells lose the ability to maintain cluster-forming cells [10]. Among the mCherry⁺ (Sox17⁺) cells, we observed to some extent GFP⁺ cells (shLuc- or sh*Rasip1*-transduced cells) (Fig. 3A, lower right panel). Required numbers of GFP⁺ cells were sorted by FACS as presented in Fig. 3B, for the analysis of *Rasip1* expression in shLuc- and sh*Rasip1*-transduced cells and/or for the colony-forming assays, respectively. The expression level of *Rasip1* was decreased by 42% in cells transduced with sh*Rasip1* as assessed by ImageJ (Fig. 3B, right panel). Moreover, we noted that Sox17-transduced cells with downregulated *Rasip1* expression by the introduction of shRNA displayed a decrease in their total and multilineage colony-forming activities (Fig. 3C). These results indicate that cells

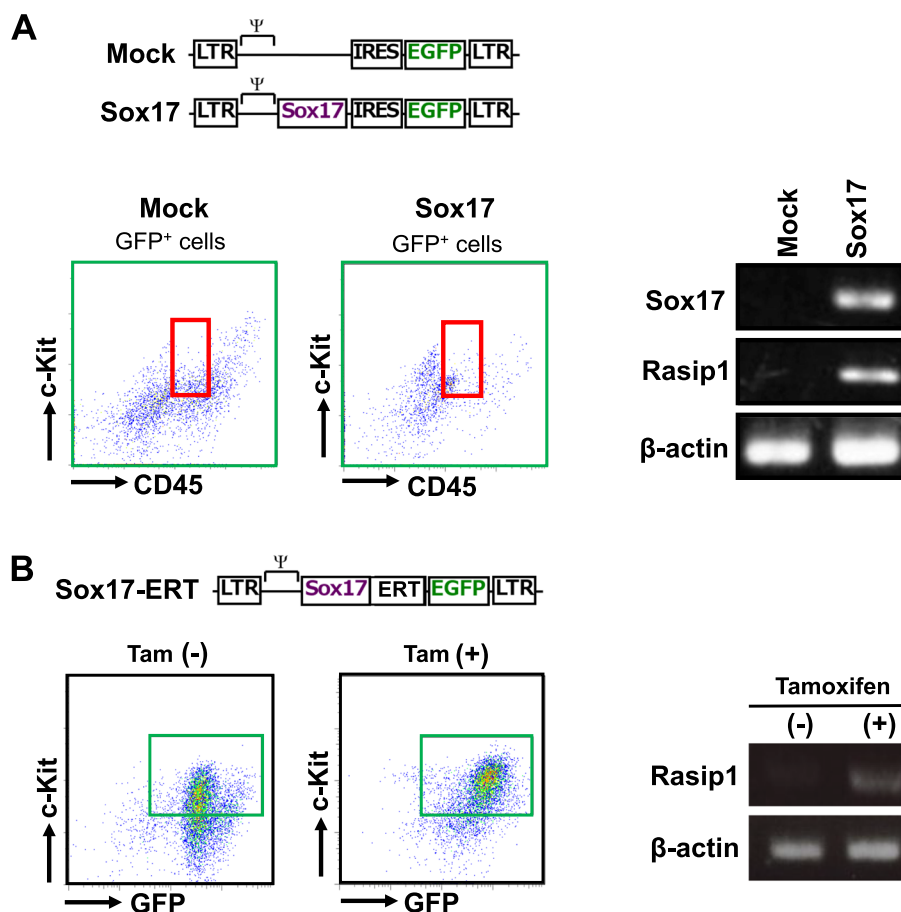


Fig. 2 Expression of Rasip1 in Sox17 (GFP)-transduced CD45^{low} c-Kit^{high} cells. **A** Upper panel: A schema of Sox17-IRES-GFP (Sox17) and IRES-GFP (Mock) retrovirus vectors. Lower panel: The red squares show a region of the CD45^{low} c-Kit^{high} cell population. The expression of Rasip1 in Mock- or Sox17-transduced cells was analyzed by RT-PCR and normalized by β-actin. **B** Upper panel: A schema of the Sox17-ERT-IRES-GFP retrovirus vector. Lower panel: The dark green squares show Sox17 (GFP)⁺ CD45^{low} c-Kit^{high} cells. After FACS sorting, expression analysis of the *Rasip1* gene was performed in Sox17-ERT-IRES-GFP-transduced cells with or without tamoxifen (1.0 μg/ml)

with knockdown of Rasip1 decreased the hematopoietic capacity in vitro.

We noticed that Rasip1-GFP expressing cells tended to form smaller clusters compared with the control (Fig. 4A, left two panels). Hence, we calculated and compared the average volume of these clusters (Fig. 4A, right panel). Interestingly, the mean volume of shRasip1-transduced

clusters was significantly lower than that of shLuc-transduced clusters. This observation supports the notion that Rasip1 is involved in the formation of cell clusters. Next, we sorted shLuc-GFP and shRasip1-GFP cells with relatively high GFP expression levels, i.e., with the relatively high expression of the sh constructs (Fig. 4B, upper left two panels). The sorted cells were subjected to RT-PCR

(See figure on next page.)

Fig. 3 Rasip1 knockdown (KD) in CD45^{low} c-Kit^{high} cells. **A** Upper panel: A schema of the position of the Rasip1 shRNA in the Rasip1 mRNA, a retrovirus vector of Sox17-IRES-mCherry, and retrovirus vectors of shLuc and shRasip1. Lower panel: After 4 days of Sox17-IRES-mCherry transduction, Sox17-transduced cells formed cell clusters. shLuc and shRasip1 were introduced into Sox17-transduced cells, and the cells were co-cultured with OP9 stromal cells. Morphologies of shRasip1 (green, GFP⁺)-transduced Sox17⁺ cells (red, mCherry⁺). Scale bar, 1.0 mm. **B** shLuc- or shRasip1-transduced GFP⁺ cells were recovered by FACS. Expression of Rasip1 in shLuc- and shRasip1-transduced cells was analyzed by RT-PCR and normalized by β-actin gene expression. RT-PCR result is in the static image that is generated by a mirror-reversal of an original across a horizontal axis, due to the sample order in the electrophoresis. **C** Sorted GFP⁺ cells (2.5 × 10³) were embedded in a semisolid medium. The number of total (CFU-C) and mix (CFU-Mix) colonies was scored after 7 days of culture. The pair of colony numbers (sh-Luc and shRasip1) in each experimental group were plotted and connected by a line. Each symbol represents the colony numbers observed with each cell preparation from individual litters of E10.5 mice (n = 7, 7 individual litters of mice from which each experimental group was set up). *p ≤ 0.05; **p ≤ 0.01

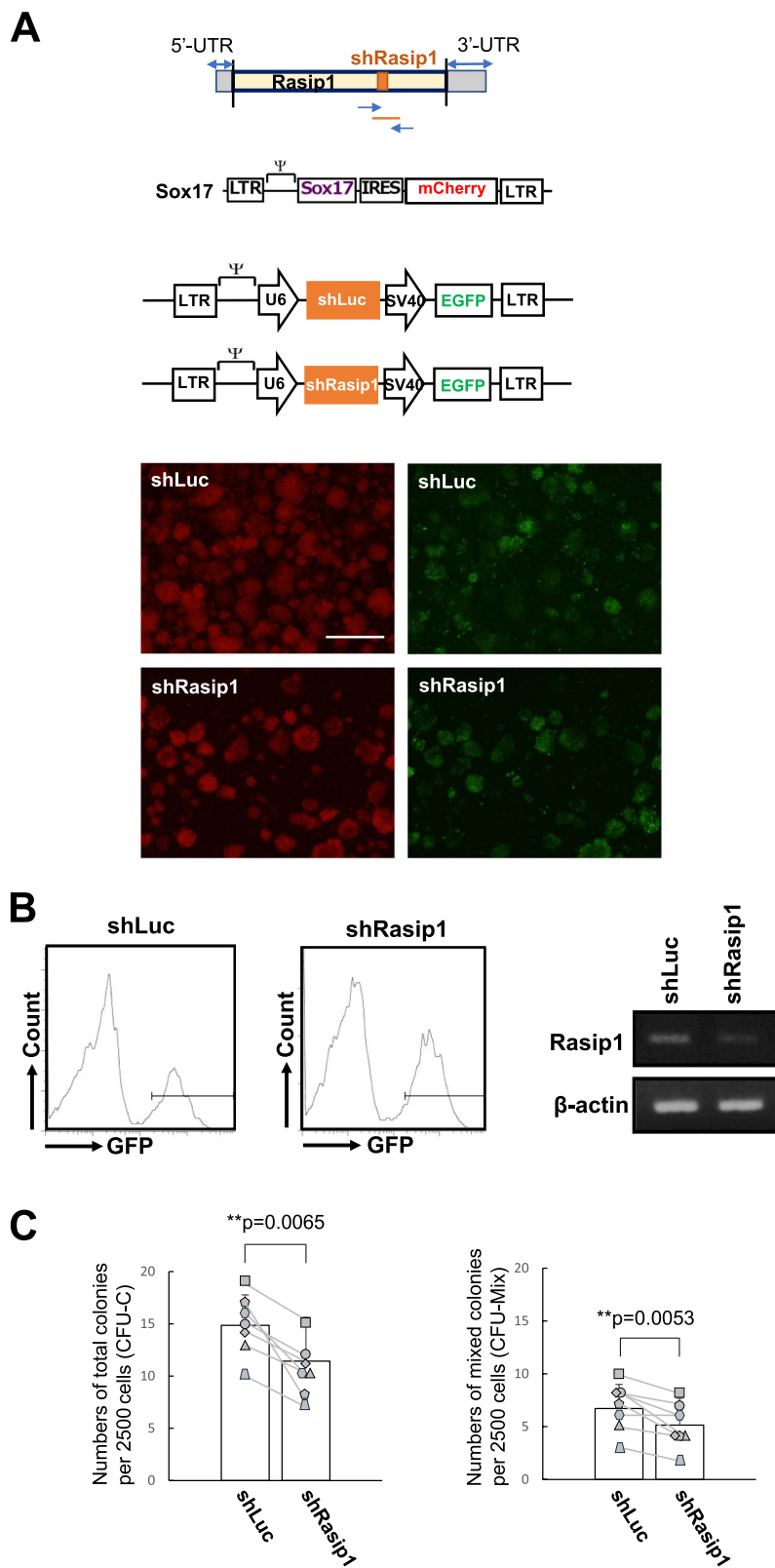


Fig. 3 (See legend on previous page.)

analysis of *Rasip1* transcripts. As shown in Fig. 4B (upper right panel), *Rasip1* expression was decreased by 36% in the sorted sh*Rasip1*-GFP high expression cells by ImageJ. In contrast, as shown in Supplementary Fig. 2A (right panel), the sorted sh*Rasip1*-GFP low expression cells showed only an 8.8% decrease in the *Rasip1* expression at the transcription level as assessed by ImageJ. Total and multilineage colony-forming activities of the cells with high expression of the *Rasip1* knockdown construct (Fig. 4B lower panels) were significantly decreased, while those of the cells with very low expression of the *Rasip1* construct (Supplementary Fig. 2B) were not decreased. This result suggests that reduction of *Rasip1* expression leads to reduction of hematopoietic activity.

***Rasip1* overexpression in CD45^{low}c-Kit^{high} cells increases the hematopoietic activity**

To assess the involvement of *Rasip1* in the hematopoietic activity of IAHCs (Fig. 5A), we tested the hematopoietic activity of *Rasip1* overexpressing cells in vitro. We transduced CD45^{low}c-Kit^{high} cells with retrovirus encoding the IRES-GFP gene (Mock) or the *Rasip1*-IRES-GFP gene (*Rasip1*) and co-cultured them with OP9 stromal cells (Fig. 5B, day 0). After 4 days of co-culture, we observed on the panel 2 populations, (1) CD45^{low}c-Kit^{high} and (2) CD45^{low}c-Kit^{low} populations, the former of which was missing in mock-transduced cells (Fig. 5C, left two panels). Cells indicated in red squares in Fig. 5C (left two panels) were embedded in the semisolid medium for colony-forming assays. As shown in Fig. 5D top two panels (colony assay 1), *Rasip1*-transduced cells displayed a significantly higher ability to form total colonies (CFU-C) and mixed colonies (CFU-Mix) compared with mock-transduced cells. Next, we examined whether this ability was maintained during the subculture of *Rasip1*-transduced cells with OP9 cells. In the subculture, after 8 days from the initial culture, cells indicated in red squares in Fig. 5C (right two panels) were sorted and subjected to colony-forming assays. As shown in Fig. 5D lower two

panels (colony assay 2), the number of total colonies (CFU-C) of *Rasip1*-transduced cells was significantly larger than that of the mock control, while the number of mixed colonies (CFU-Mix) of *Rasip1*-transduced cells was statistically insignificant as compared with the mock control. Cells transduced with *Rasip1* maintained their multipotent colony-forming activity for at least 7 days. Therefore, these results indicate that *Rasip1*, a *Sox17* downstream target gene, endows *Sox17*-untransduced CD45^{low}c-Kit^{high} AGM cells with the capacity to maintain hematopoietic activity, although it is transient.

Discussion

This report provides the first evidence that *Rasip1* is a novel *Sox17* downstream target gene and proposes the idea that *Rasip1* contributes to the maintenance of the property of IAHCs of the E10.5 AGM region. *Rasip1* is here shown to be expressed in most part of the c-Kit⁺ and *Sox17*⁺ cells in IAHCs and endothelial cells. This may be related to a previously reported function of *Rasip1*, a vascular-specific regulator [34–36], which is interesting in the sense that HSCs arise from the hemogenic endothelium of the dorsal aorta [10]. *Rasip1* is expressed in *Sox17*-transduced CD45^{low}c-Kit^{high} cells which contain HSC and HPC. From the luciferase assay, *Sox17*-induced *Rasip1* expression required the most proximal *Sox17*-binding site (*Rasip1* [5]) of the *Rasip1* gene enhancer region. Moreover, the ChIP assay results indicate that *Sox17* directly binds to this site. Functionally, downregulation of *Rasip1* in *Sox17*-transduced CD45^{low}c-Kit^{high} cells leads to the inhibition of the multilineage colony-forming ability, while upregulation of *Rasip1* causes the increase of the colony-forming ability. Our study indicates the idea that *Sox17* positively regulates hematopoiesis at least in part through *Rasip1* expression in IAHCs, which arises from endothelial cells as depicted in Fig. 6.

Rasip1 was reported as an endothelial cell-specific regulator of GTPase signaling, cell architecture, and

(See figure on next page.)

Fig. 4 *Rasip1* knockdown (KD) in *Sox17*-transduced CD45^{low}c-Kit^{high} cells. **A** Morphologies of GFP⁺ cell clusters. Yellow arrowheads indicate cell clusters which expressed in bright green color (GFP⁺ with high intensity). The bar graph shows the average volume and standard deviation ($n = 3$, 3 individual litters of mice from which each experimental group was set up). Scale bar, 200 μ m. The average volume of cell clusters with high GFP expression in each group (shLuc and sh*Rasip1*) was measured and analyzed as follows: (1) we measured the longest diameter and perpendicular diameter with the longest diameter; (2) we calculated the average volume as follows: cluster volume = length \times width²/2, where length represents the largest cluster diameter and width represents the perpendicular diameter with the longest diameter; (3) we calculated the average volumes of 10 clusters in maximum in one individual experiment; (4) we calculated the total average volume of all 3 experiments ($n = 3$, 3 individual litters of mice from which each experimental group was set up). **B** Upper panels: shLuc- or sh*Rasip1*-transduced cells with relatively high GFP⁺ expression levels, i.e., with the relatively high expression of the sh constructs were recovered by FACS. As indicated in the FACS profile, the dark green squares show the high GFP⁺ cell population. Expression of *Rasip1* in shLuc- and sh*Rasip1*-transduced cells was analyzed by RT-PCR and normalized by β -actin gene expression. RT-PCR result is in the static image that is generated by a mirror reversal of an original across a horizontal axis, due to the sample order in the electrophoresis. Lower panels: Sorted GFP⁺ cells (3.0×10^3) were embedded in a semisolid medium. The number of total (CFU-C) and multilineage (CFU-Mix) colonies were scored after 7 days of culture. The pair of colony numbers (sh-Luc and sh*Rasip1*) in each experimental group were plotted and connected by a line. Each symbol represents the colony numbers observed with each cell preparation from individual litters of E10.5 mice ($n = 4$, 4 individual litters of mice from which each experimental group was set up). * $p \leq 0.05$

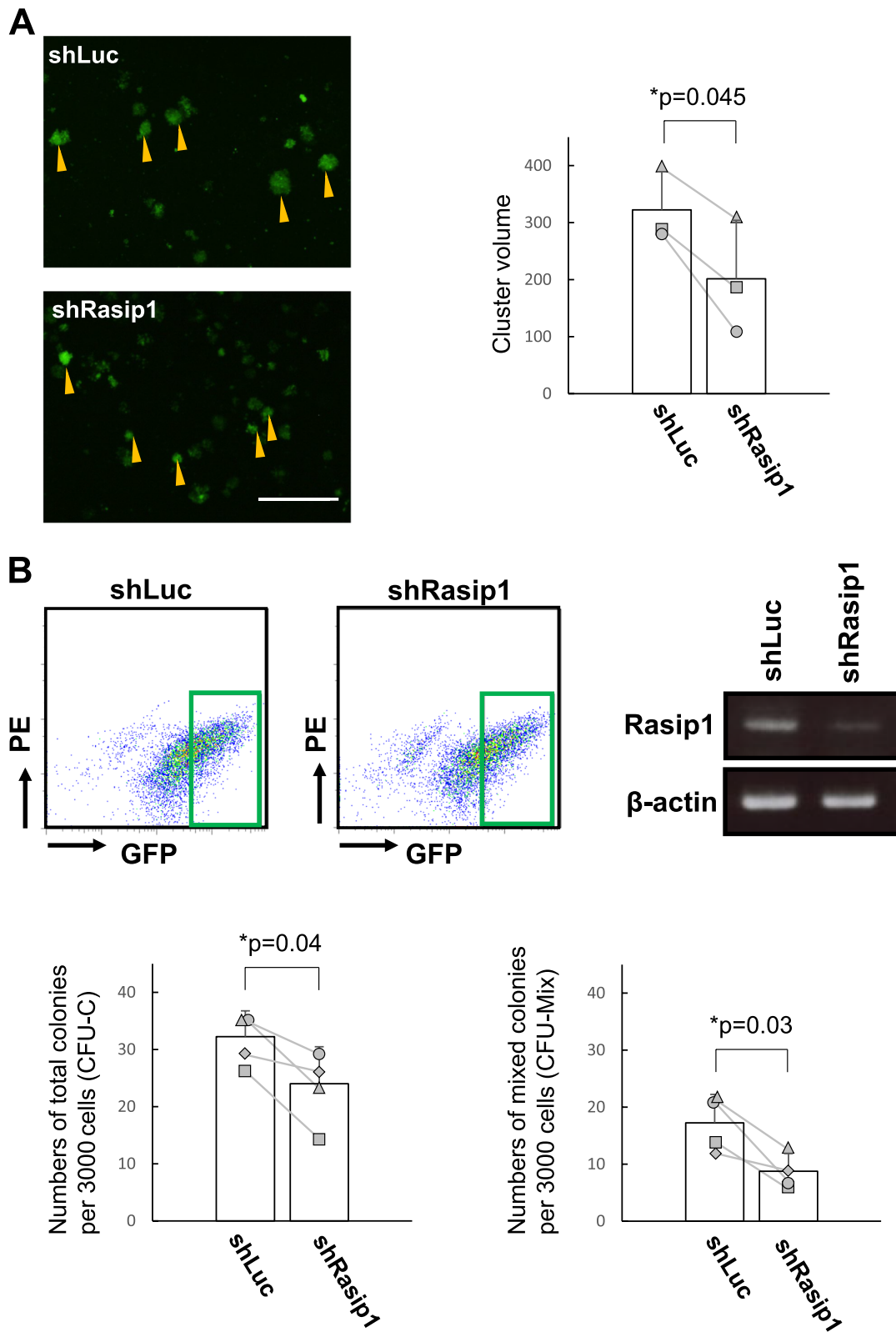


Fig. 4 (See legend on previous page.)

adhesion, which is essential for endothelial cell morphogenesis and blood vessel tubulogenesis [34–36, 38, 39]. Mitin et al. reported the identification of Rasip1 which displays the characteristics of an endomembrane Ras effector [40]. Their experiments showed that Rasip1 possesses a Ras-associating domain (RA), which is homologous to the RA domains of other Ras “effectors,” and that Rasip1 binds to the GTP-loaded form of Ras, both in vitro and in vivo [40]. Components of the Ras signaling pathway are important during embryonic vasculogenesis and angiogenesis [40]. It was previously reported that the Ras-MAPK pathway is important for the emergence of IAHCs from the hemogenic endothelial cells [41]. Overexpression of a dominant negative form of Ras in the primary culture of the AGM region was shown to inhibit the production of hematopoietic cells [41]. Taken together, we speculate that Rasip1 may well be associated with the maintenance of hematopoietic cell clusters with the hematopoietic activity via binding to Ras as an effector of the Ras signaling. Xu et al. reported that the *Rasip1* gene is significantly expressed in vascular endothelial cells throughout development [39]. *Rasip1* expression is undetectable in *VEGFR2* null embryos, which lack endothelial cells, suggesting that *Rasip1* is specifically expressed in endothelial cells [39]. Rasip1 is essential for embryonic vessel formation and maintenance, but not in adult vessels [38]. Together, these data suggest that Rasip1 is an endothelial factor that plays a role in vascular development. Rasip1 continued to be expressed in the endothelium of vessels into the postnatal stages and was detected in adult organs, particularly in the vascularized lung [40]. Previous studies reported that Rasip1 knockout mice had formed patent lumens [36]. At E9.0, *Rasip1*^{-/-} embryos exhibited a small size, pale, hemorrhage, and pericardial edema [34]. At E10.5, *Rasip1*^{-/-} embryos were markedly smaller than control littermates with severe edema and hemorrhage. Viable *Rasip1*^{-/-} embryos were not detected past E10.5 [36]. Taken together, they concluded that targeted disruption of mouse *Rasip1* results in abnormal cardiovascular development and midgestational lethality [36]. From these data, we predict that the absence of Rasip1 in vivo disrupts the development of blood vessels including the dorsal aorta of the AGM region where the hemogenic endothelial cells reside and will eventually prevent the emergence of hematopoietic clusters from

hemogenic endothelium and furtherly fail the development of embryonic hematopoiesis.

The IAHC cells express adherent molecules, which are VE-Cad and CD31, on the membrane side of the endothelial cells in the dorsal aorta [5, 23]. In Fig. 1B, whole-mount immunostaining images show that IAHCs express CD31 and Rasip1 on the membrane of IAHC cells. In Table 1, other top selected genes such as endothelial cell-specific *Emcn*, *Plvap*, and *Cldn5* which are involved in blood vessel development or tight junction, and *ESAM* which is involved in adhesion molecule activation, are targets of Sox17 transcription factor. Rasip1 appears to regulate endothelial cell–cell junction in a mode different from that of cell adhesion molecule, suggesting that Rasip1 alters junctional actin organization [36]. Post et al. revealed that Rap1 is associated with a small GTPase regulating cell–cell adhesion, cell–matrix adhesion, and actin rearrangements, and all processes dynamically coordinate during cell spreading and endothelial barrier function [32]. At cell–cell contacts, Rasip1, in conjunction with the Rap1 effector ras-association and dilute domain-containing protein (Radil), suppresses RhoA/ROCK signaling via the RhoA, RhoGAP, and ArhGAP29 [33, 35]. The Rasip1-ArhGAP29 pathway functions in Rap1-mediated regulation of endothelial junctions, which controls endothelial barrier function [30]. In this process, Rasip1 cooperates with its close relative Radil to inhibit Rho-mediated stress fiber formation and induce junctional tightening [33]. Moreover, it was reported that Heart of Glass 1 (HEG1), a transmembrane receptor that is essential for cardiovascular development, binds directly to Rasip1. Rasip1 localizes forming endothelial cell (EC) cell–cell junctions, and silencing HEG1 prevents this localization. These studies established that the binding of HEG1 to Rasip1 mediates Rap1-dependent recruitment of Rasip1 to and stabilization of EC cell–cell junctions [35]. HEG1 is required for Rasip1 translocation to cell–cell contacts. However, the formation of a Rasip1-Rap1 or Rasip1-Radil-ARHGAP29 complex is not dependent on the presence of HEG1. From these reports, we speculate that Rasip1 has a regulatory effect on cluster integrity as a Sox17-downstream regulator of cell adhesion and cell–cell junction.

We already know that Rasip1 is endothelial-specific and essential for embryonic vascular development [36, 38]. In

(See figure on next page.)

Fig. 5 Rasip1 overexpression (OE) in CD45^{low}c-Kit^{high} cells. **A** A schema of IRES-GFP (Mock) and Rasip1-IRES-GFP retrovirus vectors. **B** Timeline of Rasip1 OE experiment. **C** Red squares show Mock- and Rasip1-transduced CD45^{low}c-Kit^{high} cells. **D** After 4 days of Mock and Rasip1 transduction, CD45^{low}c-Kit^{high} cells (2.5×10^2) were embedded in a semisolid medium (colony assay 1). According to the timeline in **B**, CD45^{low}c-Kit^{high} cells were sorted (5.0×10^2) after 8 days of Rasip1 transduction (Colony assay 2). The number of total (CFU-C) and multilineage (CFU-Mix) colonies was scored after 7 days of culture ($n=5$). The pair of colony numbers (Mock and Rasip1) in each experimental group were plotted and connected by a line. Each symbol represents the colony numbers observed with each cell preparation from individual litters of E10.5 mice ($n=6$, 6 individual litters of mice from which each experimental group was set up). * $p \leq 0.05$

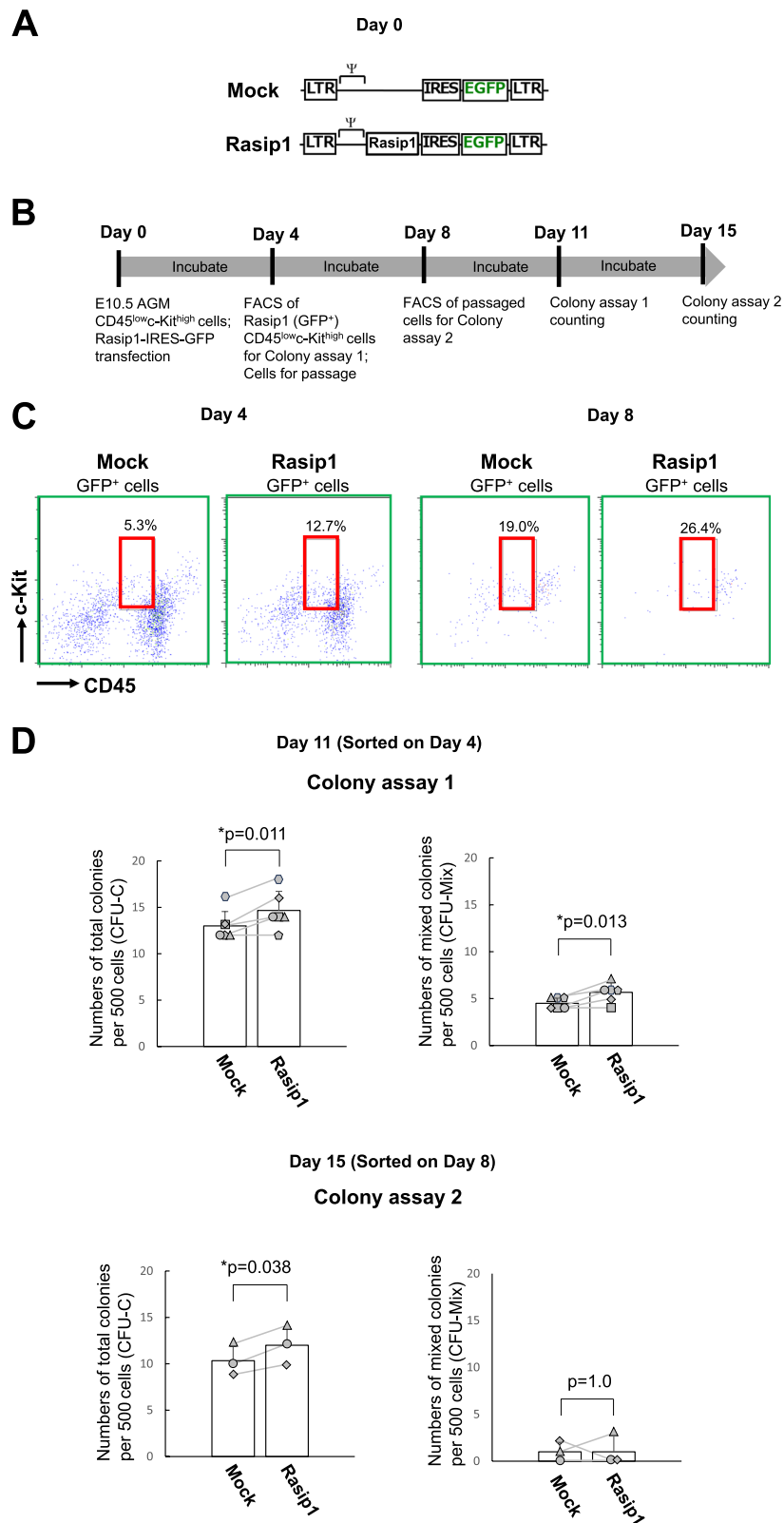


Fig. 5 (See legend on previous page.)

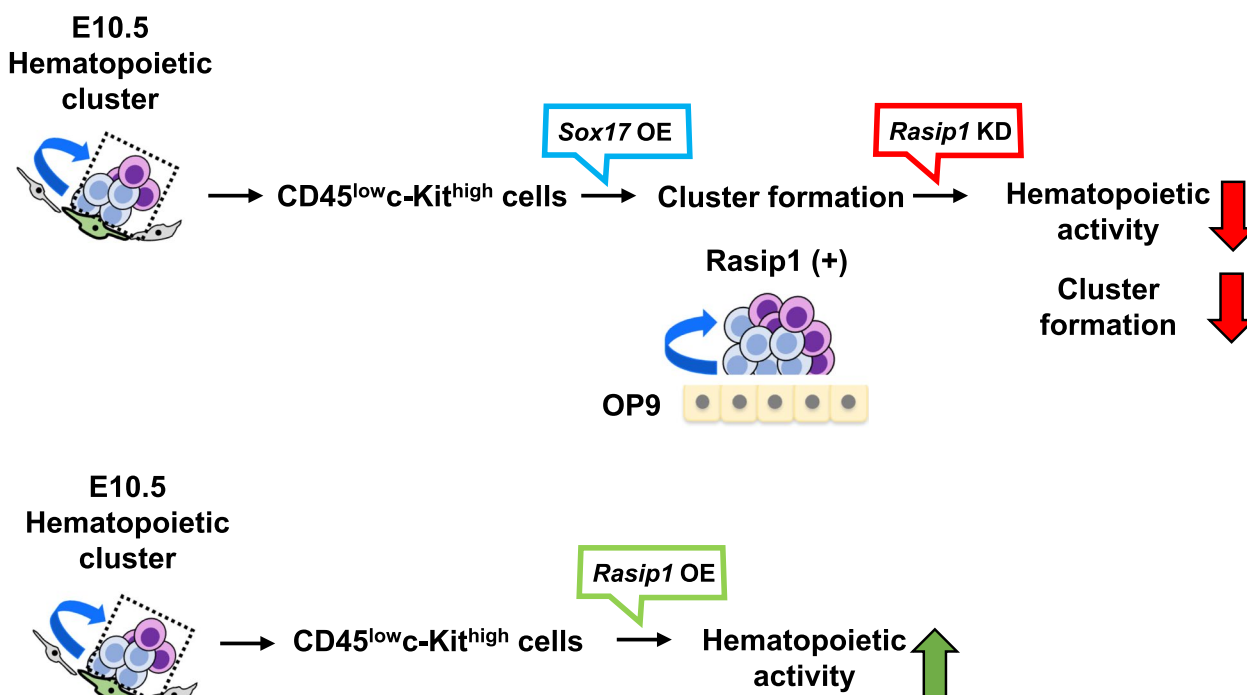


Fig. 6 Formation of IAHCs involving Rasip1. A model of Rasip1 function in IAHCs. Sox17 induces the expression of Rasip1 which eventually leads to the hematopoietic activity of HSCs in IAHCs. Upper panel: Function of Rasip1 revealed by knockdown experiments. Forced expression of Sox17 (*Sox17* OE) in CD45^{low}c-Kit^{high} cells was known to maintain the formation of hematopoietic cell clusters. However, the downstream signaling involved remained poorly understood. A current study has revealed that Rasip1 knockdown (*Rasip1* KD) decreases hematopoietic activity and cluster formation. Lower panel: Effect of Rasip1 overexpression (*Rasip1* OE) in CD45^{low}c-Kit^{high} cells. *Rasip1* OE leads to a significant but transient increase in the hematopoietic activity, suggesting the presence of a cooperating factor for sustained hematopoietic activity

addition to this previous report, we found out that Rasip1 has a role in contributing to maintaining the hematopoietic activity and cluster formation of Sox17-transduced CD45^{low}c-Kit^{high} cells. As shown in Fig. 4A, we have assessed the volume of GFP⁺ cluster cells with high intensity. From the result, the volume of clusters of cells with high GFP intensity in the Rasip1 knockdown group was decreased when compared with the control. In previous reports, Sox17-transduced cells highly expressed adherent molecules to form cell clusters and genes associated with the hematopoietic capacity to maintain the undifferentiated state of HSC-containing cluster cells [4]. In the scheme of mouse chromosome 7 where the *Rasip1* is located (Fig. 1C), we observed the putative Sox17-binding site (5), which is found to be located downstream before the *Izumo1* gene that encodes Izumo1 protein, activates the *Rasip1* gene expression. Functionally, Izumo1 has a different physiological role than Rasip1. In mammalian fertilization, Izumo1 binds to its egg receptor counterpart, Juno also known as folate receptor 4, to facilitate recognition and fusion of the gametes. Still, there were no reports of the interplay between the *Izumo1* gene and *Sox17* transcription factor in RNA sequence data of highly expressed genes of the Sox17. Additionally, our study shows that the *Rasip1* upregulation

in vitro maintains IAHCs in an undifferentiated state, although for a short period in vitro. However, it is not fully understood how Rasip1 contributes to the hematopoietic activity of IAHC cells and what factors cooperate with Rasip1 for long-term maintenance of such activity.

In this study, we have shown that a Sox17-downstream target Rasip1 contributes to cluster formation and the hematopoietic activity of IAHC cells in the E10.5 AGM region of the midgestation mouse embryo.

Conclusion

In summary, Rasip1 is identified as a Sox17 downstream gene and found to upregulate, although transient, the hematopoietic activity of HSC-containing IAHC cells of the dorsal aorta's AGM region in midgestation (E10.5) mouse embryo.

Abbreviations

HSCs	Hematopoietic stem cells
IAHCs	Intra-aortic hematopoietic cell clusters
AGM	Aorta-gonad-mesonephros
HSPCs	Hematopoietic stem/progenitor cells
E	Embryonic day
DMEM	Dulbecco's Modified Eagle's medium

RT-PCR	Reverse transcription-polymerase chain reaction
Tam	Tamoxifen
shRNA	Short hairpin RNA
Luc	Luciferase
FACS	Fluorescence-activated cell sorting
VE-cad	Vascular-endothelial cadherin
ESAM	Endothelial-specific adhesion molecule
Notch1	Neurogenic locus notch homolog protein 1
IRES	Internal ribosome entry site
GFP	Green fluorescent protein

Supplementary Information

The online version contains supplementary material available at <https://doi.org/10.1186/s41232-023-00292-4>.

Additional file 1: Supplementary Table S1. Expression levels of genes examined in the Sox17 (GFP)⁺ CD45^{low}c-Kit^{high} cells and the Sox17 (GFP)⁻ CD45^{low}c-Kit^{high} cells from the same set of E10.5 Sox17-GFP embryos. The values of FPKM+1 were used to calculate the ratio of gene expression levels between the Sox17 (GFP)⁺ CD45^{low}c-Kit^{high} cells and the Sox17 (GFP)⁻ CD45^{low}c-Kit^{high} cells. FPKM: fragments per kilobase of transcript per million mapped reads.

Additional file 2: Supplementary Fig. 1. A. Gel analysis of enzymatic digestion (original gel image of Fig. 1E). B. Chip assay (original gel image of Fig. 1F). **Supplementary Fig. 2.** A. shRasip1-IRES-GFP correlates with Rasip1 KD efficiency. shLuc- or shRasip1-transduced GFP⁺ cells were recovered by FACS. As indicated in the FACS profile, the light green squares show a GFP⁺ cell population with lower expression i.e. with the lower expression of the sh constructs. Expression level of Rasip1 in shLuc- and shRasip1-transduced cells was analyzed by RT-PCR and normalized by β -actin gene expression. RT-PCR result is in the static image that is generated by a mirror-reversal of an original across a horizontal axis, due to the sample order in the electrophoresis. B. Sorted GFP⁺ cells (3.0×10^3) were embedded in a semisolid medium. The number of total (CFU-C) and multilineage (CFU-Mix) colonies were scored after 7 days of culture. The pair of colony numbers (sh-Luc and shRasip1) in each experimental group were plotted and connected by a line. Each symbol represents the colony numbers observed with each cell preparation from individual litters of E10.5 mice ($n=4$, 4 individual litters of mice from which each experimental group was set up). * $p \leq 0.05$.

Acknowledgements

We thank Dr. T. Nakano for the OP9 cells, Ms. K. Inoue for technical assistance, and Ms. M. Makino for secretarial assistance. We also thank Ms. H. Saito to prepare Sox17^{GFP/+} mouse embryos.

Authors' contributions

GM, IN, KS, RT, AI, YK, and MK conducted the in vivo and in vitro experiments. GM, IN, and TT planned the experiments. MA, MO, and AI performed RNA sequencing analysis. GM, IN, and TT wrote the manuscript. All authors read and approved the final manuscript.

Authors' information

The present address of Kiyoka Saito is Laboratory of Proteostasis in Stem Cell, International Research Center for Medical Sciences, Kumamoto University, 2-2-1 Honjo, Chuo-ku, Kumamoto 860-0811, Japan. The present address of Ayumi Itabashi is the Department of Immunology, Graduate School of Medicine and Faculty of Medicine, University of Tokyo, 7-3-1, Hongo, Bunkyo-ku, Tokyo 113-0033, Japan. The present address of Mitsujiro Osawa is Thyas Co. Ltd., Kyoto 606-8501, Japan.

Funding

This work was supported by grants from the Ministry of Education, Culture, Sports, Science and Technology of Japan [26440118 and 18K06249 (I. N.), 22130008, 15H04292, and 18H02678 (T. T.)], Nanken-Kyoten, TMDU (Grant numbers: H26-A39, H27-A35, H28-A11, 2020-kokunai-41, 2021-kokunai-25, 2022-kokunai-09, 2023-kokunai-10).

Availability of data and materials

RNA-sequencing data were deposited in the DNA Data Bank of Japan with the accession no. DRR398016 (Sox17 (+) IAHC cells: Sox17 (GFP)⁺ CD45^{low}c-Kit^{high} cells) and DRR398017 (Sox17 (-) IAHC cells: Sox17 (GFP)⁻ CD45^{low}c-Kit^{high} cells). Further information and requests for resources and reagents should be directed to the authors: Ikuo Nobuhisa (nobuhisa@nakamura-u.ac.jp) and Tetsuya Taga (taga.scr@mri.tmd.ac.jp).

Declarations

Ethics approval and consent to participate

Animal experiments were performed under institutional guidelines approved by the Animal Care Committee of Tokyo Medical and Dental University (approval numbers: A2018-265C, A2019-108C, A2021-177C, A2023-146A).

Consent for publication

Not applicable.

Competing interests

The authors declare that they have no competing interests.

Author details

¹Department of Stem Cell Regulation, Medical Research Institute, Tokyo Medical and Dental University (TMDU), 1-5-45 Yushima, Bunkyo-Ku, Tokyo 113-8510, Japan. ²Department of Nutritional Sciences, Faculty of Nutritional Sciences, Nakamura Gakuen University, 5-7-1, Befu, Jonan-Ku, Fukuoka 814-0198, Japan. ³Department of Veterinary Anatomy, Graduate School of Agricultural and Life Science, University of Tokyo, 1-1-1, Yayoi, Bunkyo-Ku, Tokyo 113-8567, Japan. ⁴Department of Experimental Animal Model for Human Disease, Center for Experimental Animals, Tokyo Medical and Dental University (TMDU), 1-5-45 Yushima, Bunkyo-Ku, Tokyo 113-8510, Japan. ⁵Department of Clinical Application, Center for iPSC Cell Research and Application (CiRA), Kyoto University, Kyoto 606-8507, Japan. ⁶Division of Stem Cell and Molecular Medicine, Center for Stem Cell Biology and Regenerative Medicine, The Institute of Medical Science, The University of Tokyo, 4-6-1 Shirokanedai, Minato-Ku, Tokyo 108-8039, Japan.

Received: 22 August 2022 Accepted: 13 July 2023

Published online: 08 August 2023

References

- Dzierzak E, Speck NA. Of lineage and legacy: the development of mammalian hematopoietic stem cells. *Nat Immunol*. 2008;9:129–36.
- Ferkowicz MJ, Yoder MC. Blood island formation: longstanding observations and modern interpretations. *Exp Hematol*. 2005;33:1041–7.
- de Bruijn MF, Speck NA, Peeters MC, Dzierzak E. Definitive hematopoietic stem cell first develops within the major arterial regions of the mouse embryo. *EMBO J*. 2000;19(11):2465–74.
- Swiers G, Rode C, Azzoni E, de Bruijn MF. A short history of hemogenic endothelium. *Blood Cells Mol Dis*. 2013;51(4):206–12.
- Yokomizo T, Yamada-Inagawa T, Yzaguirre AD, Chen MJ, Speck NA, Dzierzak E. Three-dimensional cartography of hematopoietic clusters in the vasculature of whole mouse embryos. *Development*. 2010;137(21):3651–61.
- Bertrand JY, Giroux S, Golub R, Claine M, Boucontet L, Godin I, Cumano A. Characterization of purified intraembryonic hematopoietic stem cells as a tool to define their site of origin. *Proc Natl Acad Sci USA*. 2005;102(1):134–9.
- Rybtsov S, Sobiesak M, Taoudi S, Souilhol C, Senserrich J, Liakhovitskaia A, Ivanovs A, Frampton J, Zao S, Medvinsky A. Hierarchical organization and early hematopoietic specification of the developing HSC lineage in the AGM region. *J Exp Med*. 2011;208(6):1305–15.
- Mizuochi C, Fraser S, Biasch K, Horio Y, Kikushige Y, Tani K, Akashi K, Taviani M, Sugiyama D. Intra-aortic clusters undergo endothelial to hematopoietic phenotypic transition during early embryogenesis. *PLoS ONE*. 2012;7(4): e35763.

9. Chen M, Yokomizo T, Ziegler B, Dzierzak E, Speck NA. Runx1 is required for the endothelial to haematopoietic cell transition but not thereafter. *Nature*. 2009;457(7231):887–91.
10. Nobuhisa I, Osawa M, Uemura M, Kishikawa Y, Anani M, Harada K, Takagi H, Saito K, Kanai-Azuma M, Kanai Y, Iwama A, Taga T. Sox17-mediated maintenance of intra-aortic hematopoietic cell clusters. *Mol Cell Biol*. 2013;34(11):1976–90.
11. Taoudi S, Gonneau C, Moore K, Sheridan JM, Blackburn CC, Taylor E, Medvinsky A. Extensive hematopoietic stem cell generation in the AGM region via maturation of VE cadherin⁺CD45⁺ pre-definitive HSCs. *Cell Stem Cell*. 2008;3(1):99–108.
12. Taoudi S, Morrison AM, Inoue H, Gribo R, Ure J, Medvinsky A. Progressive divergence of definitive hematopoietic stem cells from the endothelial compartment does not depend on contact with the fetal liver. *Development*. 2005;132(18):4179–91.
13. Nobuhisa I, Otsu N, Okada S, Nakagata N, Taga T. Identification of a population of cells with hematopoietic stem cell properties in mouse aorta-gonad-mesonephros cultures. *Exp Cell Res*. 2007;313(5):965–74.
14. Otsu N, Nobuhisa I, Mochita M, Taga T. Inhibitory effects of homeodomain-interacting protein kinase 2 on the aorta-gonad-mesonephros hematopoiesis. *Exp Cell Res*. 2007;313(1):88–97.
15. Mukoyama Y, Hara T, Xu M, Tamura K, Donovan PJ, Kim H, Kogo H, Tsuji K, Nakahata T, Miyajima A. In vitro expansion of murine multipotential hematopoietic progenitors from the embryonic aorta-gonad-mesonephros region. *Immunity*. 1998;1:105–14.
16. Nobuhisa I, Yamasaki S, Ramadan A, Taga T. CD45^{low}c-Kit^{high} cells have hematopoietic properties in the mouse aorta-gonad mesonephros region. *Exp Cell Res*. 2012;318(6):705–15.
17. Saito K, Nobuhisa I, Harada K, Takahashi S, Anani M, Lickert H, Kanai-Azuma M, Kanai Y, Taga T. Maintenance of hematopoietic stem and progenitor cells in fetal intra-aortic hematopoietic clusters by Sox17-Notch1-Hes1 axis. *Exp Cell Res*. 2018;365(1):145–55.
18. Tam P, Kanai-Azuma M, Kanai Y. Early endoderm development in vertebrates: lineage differentiation and morphogenetic function. *Curr Opin Genet Dev*. 2003;13(4):393–400.
19. Yasunaga M, Tada S, Torikai-Nishikawa S, Nakano Y, Okada M, Jakt LM, Nishikawa S, Chiba T, Era T, Nishikawa S. Induction and monitoring of definitive and visceral endoderm differentiation of mouse ES cells. *Nat Biotechnol*. 2005;23(12):1542–50.
20. Kanai-Azuma M, Kanai Y, Gad JM, Tajima Y, Taya C, Kurohmaru M, Sanai Y, Yonehara H, Yazaki K, Tam PPL, Hayashi Y. Depletion of definitive gut endoderm in Sox17-null mutant mice. *Development*. 2002;129(10):2367–79.
21. Clarke R, Yzaguirre A, Yashiro-Ohtani Y, Bondue A, Blanpain C, Pear W, Speck NA, Keller G. The expression of Sox17 identifies and regulates hemogenic endothelium. *Nat Cell Biol*. 2013;15(5):502–10.
22. Kumano K, Chiba S, Kunisato A, Sata M, Saito T, Nakagami-Yamaguchi E, Yamaguchi T, Masuda S, Shimizu K, Takahashi T, Ogawa S, Hamada Y, Hirai H. Notch1 but not Notch2 is essential for generating hematopoietic stem cells from endothelial cells. *Immunity*. 2003;18(5):699–711.
23. Takahashi S, Nobuhisa I, Saito K, Melig G, Itabashi A, Harada K, Osawa M, Endo TA, Iwama A, Taga T. Sox17-mediated expression of adherent molecules is required for the maintenance of undifferentiated hematopoietic cluster formation in the midgestation mouse embryo. *Differentiation*. 2020;115:53–61.
24. Harada K, Nobuhisa I, Anani M, Saito K, Taga T. Thrombopoietin contributes to the formation and the maintenance of hematopoietic progenitor-containing cell clusters in the intra-gonad-mesonephros region. *Cytokine*. 2017;95:35–42.
25. Anani M, Nobuhisa I, Osawa M, Iwama A, Harada K, Saito K, Taga T. Sox17 as a candidate regulator of myeloid restricted differentiation potential. *Dev Growth Differ*. 2014;56:46979.
26. Kayamori K, Nagai Y, Zhong C, Kaito S, Shinoda D, Koide S, Kuribayashi W, Oshima M, Nakajima-Takagi Y, Yamashita M, Mimura N, Becker HJ, Izawa K, Yamazaki S, Iwano S, Miyawaki A, Ito R, Tohyama K, Lennox W, Sheedy J, Weetall M, Sakaida E, Yokote K, Iwama A. DHODH inhibition synergizes with DNA-demethylating agents in the treatment of myelodysplastic syndromes. *Blood Adv*. 2021;5(2):438–50.
27. Kim I, Saunders TL, Morrison SJ. Sox17 dependence distinguishes the transcriptional regulation of fetal from adult hematopoietic stem cells. *Cell*. 2007;130(3):470–83.
28. He S, Kim I, Lim MS, Morrison SJ. Sox17 expression confers self-renewal potential and fetal stem cell characteristics upon adult hematopoietic progenitors. *Genes Dev*. 2011;25(15):1613–27.
29. Morita S, Kojima T, Kitamura T. Plat-E: an efficient and stable system for transient packaging of retroviruses. *Gene Ther*. 2000;7(12):1063–6.
30. Nakajima-Takagi Y, Osawa M, Oshima M, Takagi H, Miyagi S, Endoh M, Endo TA, Takayama N, Eto K, Toyoda T, Koseki H, Nakauchi H, Iwama A. Role of SOX17 in hematopoietic development from human embryonic stem cells. *Blood*. 2013;121(3):447–58.
31. Brummelkamp TR, Bernards R, Agami R. A system for stable expression of short interfering RNAs in mammalian cells. *Science*. 2002;296(5567):550–3.
32. Wu W, Bi C, Credille KM, Manro JR, Peek VL, Donoho GP, Yan L, Wijsman JA, Yan SB, Walgren RA. Inhibition of tumor growth and metastasis in non-small cell lung cancer by LY2801653, an inhibitor of several oncokinases, including MET. *Clin Cancer Res*. 2013;19(20):5699–710.
33. Post A, Pannekoek WJ, Ross SH, Verlaan I, Brouwer PM, Bos JL. Rasip1 mediates Rap1 regulation of Rho in endothelial barrier function through ArhGAP29. *Proc Natl Acad Sci USA*. 2013;110(28):11427–32.
34. Xu K, Sacharidou A, Fu S, Chong DC, Skaug B, Chen ZJ, Davis GE, Cleaver O. Blood vessel tubulogenesis requires Rasip1 regulation of GTPase signaling. *Dev Cell*. 2011;19(20):526–39.
35. Kreuk BJ, Gingras AJ, Knight J, Liu J, Gingras AC, Ginsberg MH. Heart of glass anchors Rasip1 at endothelial cell-cell junctions to support vascular integrity. *Elife*. 2016;5: e11394.
36. Wilson CW, Parker LH, Hall CJ, Smyczek T, Mak J, Crow A, Posthuma G, De Mazière A, Sagolla M, Chalouni C, Vitorino P, Roose-Girma M, Warming S, Klumperman J, Crosier PS, Ye W. Rasip1 regulates vertebrate vascular endothelial junction stability through Epac1-Rap1 signaling. *Blood*. 2013;122(22):3678–90.
37. Clark SC, Chereji RV, Lee PR, Fields RD, Clark DJ. Differential nucleosome spacing in neurons and glia. *Neurosci Lett*. 2020;714: 134559.
38. Koo Y, Barry DM, Xu K, Tanigaki K, Davis GE, Mineo C, Cleaver O. Rasip1 is essential to blood vessel stability and angiogenic blood vessel growth. *Angiogenesis*. 2016;2:173–90.
39. Xu K, Chong DC, Rankin SA, Zorn AM, Cleaver O. Rasip1 is required for endothelial cell motility, angiogenesis, and vessel formation. *Dev Biol*. 2009;329(2):269–79.
40. Mitin NY, Ramocki MB, Zullo AJ, Der CJ, Konieczny SF, Taparowsky EJ. Identification and characterization of rain, a novel Ras-interacting protein with a unique subcellular localization. *J Biol Chem*. 2004;279(21):22353–6.
41. Nobuhisa I, Kato R, Inoue H, Takizawa M, Okita K, Yoshimura A, Taga T. Spred-2 suppresses aorta-gonad-mesonephros hematopoiesis by inhibiting MAP kinase activation. *J Exp Med*. 2004;199(5):737–42.

Publisher's Note

Springer Nature remains neutral with regard to jurisdictional claims in published maps and institutional affiliations.

Ready to submit your research? Choose BMC and benefit from:

- fast, convenient online submission
- thorough peer review by experienced researchers in your field
- rapid publication on acceptance
- support for research data, including large and complex data types
- gold Open Access which fosters wider collaboration and increased citations
- maximum visibility for your research: over 100M website views per year

At BMC, research is always in progress.

Learn more biomedcentral.com/submissions

